# MODELLING POST-TENSIONED PRECAST CONCRETE SEGMENTAL GIRDER BRIDGES WITH DRY KEYED JOINTS – PRELIMINARY RESULTS

**EDVIS SEJKATI 1,2**

**XIANGMING ZHOU 1**

**RABEE SHAMASS 1**

**GIUSEPPE MANCINI 2**

1 Brunel University London

United Kingdom

2 Polytechnic University of Turin

Italy

**ABSTRACT:** Precast concrete segmental bridges (PCSBs) have been the most common design technology used in the last decades. It is widely recognized that segmental bridges have better durability, lower life-cycle costs and higher quality for maintenance than other types of bridges. PCSBs with externally prestressed tendons have become very popular in construction because of economical and safety reasons, fast and practical construction, and outstanding serviceability. Moreover, external tendons technique is widely used because it allows to inspect the cables and to replace them or to reinforce the tendons in case of damage while such kinds of actions are difficult to be taken in case of internal prestressing. Therefore, box section is the most common solution due to its aesthetic appeal and elegance that reduces the environmental impact as well due to the convenient maintenance for the tendons. Besides, the hollow concrete box segment can be used for service/electrical cable ducts for bridges. However, there is lack of reliable computational model for analysing behaviour of post-tensioned PCSBs. This research investigates the behaviour of PCSBs with dry keyed joints and external tendons up to failure with the use of finite element method which is validated by comparing experimental results. Deflection, joint opening, tendon slip, stresses of the tendons and the concrete are obtained from numerical analysis with recommendation on further development towards a more accurate numerical model for PCSBs made.

**Keywords:** Dry joint; Keyed joint; Joint opening; Precast concrete segmental bridge; Post-tensioned; Tendon slip

**Authors:** Edvis Sejkati; Xiangming Zhou; Rabee Shamass; Giuseppe Mancini

**Mr Edvis Sejkati** holds an MSc degree in Civil Engineering. He has research interests on seismic behaviour of civil structures and post-tensioned precast concrete segmental bridges.
**Dr Xiangming Zhou** is a Reader in Civil Engineering Design at Brunel University London. He has published extensively on concrete science, technology, mechanics and structures.
**Mr Rabee Shamass** is a PhD candidate at Brunel University London. He has research interests on modelling of keyed joints of precast concrete segmental bridges.
**Prof Giuseppe Mancini** is a professor in structural engineering at Polytechnic University of Turin. He has extensive research on concrete structures including concrete bridges.

## LITERATURE REVIEW

PCSBs are a newly developed bridge construction commonly used during the last decades. The fast construction speed and reduced need to interrupt traffic during construction are the main advantages. Differently from the monolithic type that has a continuous reinforcement in longitudinal direction, the precast segmental type consists in short elements, which are assembled together with externally prestressed tendons through keyed joints rather than continuous reinforcement. Different from pre-tensioned concrete structures, post-tensioning technique is used in PCSBs and the tendons are run outside the original concrete section and its layout cannot follow the parabolic shape. Rather it is linear between two deviation points. With this technique the structure can be prestressed in-situ without the need of transporting to construction site pre-tensioned structural elements, which may be very long, made in factory. Externally prestressed concrete has the advantage, i.e. it allows the maintenance, replacement and strengthening of the tendons. However this is little numerical model available in literature for analysing behaviour of PCSBs with keyed joints.

Ramos and Aparicio [6] proposed a numerical model taking into account material non-linearity of concrete by updating the stiffness matrix at every iteration step, using rigid links between the end nodes of the tendons and the nodes of the bridge structure where the prestressed elements are anchored, and linear elements between the segments of the joint. They obtained very similar results of load-deflection and load-prestressing force curves to experimental ones. However, the model was applied to compare the results of beam test that has much smaller dimensions than a box section of a PCSB in the field. Tandler [7] developed a numerical model by using Abaqus. The results obtained from the model have been compared with the results of Takebayashi T. et al. [5]. He assumed the free slipping of the tendons at the deviator blocks. However, instead of having a lower ultimate load than the actual one as can be expected from the free slipping assumption [6], the results show that the bridge fails at a higher mid-span applied moment. Moreover, the maximum deflection and the maximum joint opening are reached not at the same location of the bridge sample tested. This is due to the position of the applied loads that was not symmetric with respect to the mid-span while the real disposal of the loads was symmetric.

Takebayashi et al. [5] conducted an experimental study on the behaviour of a full span of a PCSB with dry joints and external tendons. The tested bridge was 44.25 m span and 10.20 m wide. The segments length was 3.40 m, except for the diaphragm segments, which were 1.725 m. The box section had a constant height of 2.40 m along the span. The two deviators at the segments 4 and 11 had the same geometry and were named D2, while the deviator at the segment 7 was named D1. The two end diaphragms were the segments 1 and 14. The bridge was prestressed with 12 external tendons: 10 of them formed from 19K15 strands and 2 from 12K15 strands protected with HDPE ducts and cement grout. The tendons are located symmetrically with respect to the longitudinal axis, but not with respect to the mid-span. Tendons from 1 to 5 (19K15) run for the whole span and they are deflected on each of the three deviators, while the tendons 6 (12K15) is anchored between the deviators D2 and it is deflected only at the deviator D1.

The table 1 shows the material properties of the tested bridge. The tested bridge was supported by elastomeric bearings. Their centres are 50 cm far away from the ends of the bridge. It was computed using back calculation that the total tendon force was 38433 kN. It also showed about 12% of losses in tendon force due to creep, shrinkage and relaxation of tendons.

Table 1 Material properties [5]

| MATERIAL | PROPERTIES ITEM | AVERAGE FIGURES [MPa] |
|---|---|---|
| Concrete | Compressive strength | 55 – 62 |
| | Modulus of elasticity | 43000 |
| Re-bars | Tensile strength | 390 |
| Tendons | Breaking strength | 1920 |
| | Modulus of elasticity | 193000 |

## NUMERICAL MODEL

### Geometry

The geometry of the original bridge has been simplified by setting the trial dimension of thickness and width of the slabs and webs, without modifying greatly the original section. The best solution found is detailed in figure 1. As aforementioned, deviators and diaphragms have different geometry from the ordinary segments. The simplified section is the same for each segment including the deviators and diaphragms.

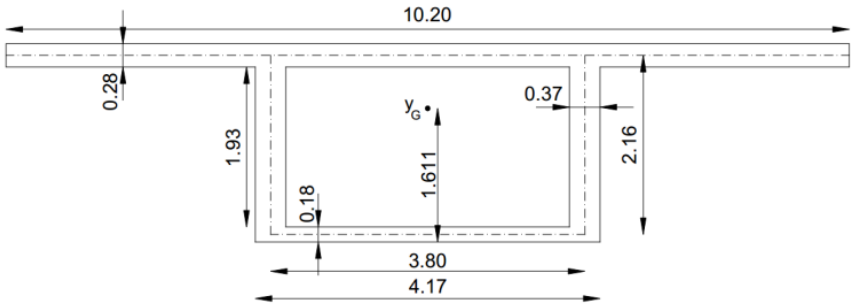


Figure 1 Simplified geometry of the original section with all dimensions in metres

### Material Properties

The analysis has been conducted up to failure for the PCSB span, therefore, a non-linear behavior of the materials has been used for this study. The elastic field is characterized by the elastic modulus and the Poisson's ratio of the material. The Von Mises plasticity model is followed which defines a yield surface that is used to compute the yielding of isotropic materials. The stress-strain relation for the steel reinforcement in the slabs and webs is elastic-perfectly plastic as suggested in EC2. The bilinear behaviour is applied for tension and compression. The value of elastic modulus $E_S$ is assumed 210 GPa and the Poisson's ratio equal to 0.28. The tensile strength of the bars is taken from the value provided by Takebayashi [5], i.e. $f_{yd} = 390\ MPa$.

The non-linear behaviour used for the tendons is similar to the reinforcing bars, except for the values and the elastic-plastic hardening model assumed. The bi-linear model is proposed in the EC2. The value of the elastic modulus of the tendons $E_p$ is 193 GPa, taken from Takebayashi's study and the Poisson's ratio is equal to 0.28 same as reinforcement steel. The breaking strength is also provided from the experimental data and is equal to

$$\frac{f_{pk}}{\gamma_s} = 1920\ MPa$$

The elastic behaviour of the concrete is defined with the Young's modulus and the Poisson's ratio as well. Takebayashi gives a range of concrete compressive strength between 55 and 62 MPa obtained from testing of samples and back calculation [5]. The lower value of the provided range has been used for the analysis. They also measured the elastic modulus of concrete equal to 43 GPa. This value is considered too high even for the upper limit of compressive strength range. Therefore, it is considered appropriate to neglect it and to compute the elastic modulus $E_c$ from the analytical relation with the concrete compressive strength given by EC2.

$$E_c = 22[(f_{cm})/10]^{0.3} = 36.689\ GPa$$

The "Concrete smeared cracking" model in Abaqus is used for modelling the concrete in this research. The smeared cracking concrete model gives a general function to model different structures, including shells as the slabs and webs of the box section [10]. Furthermore, it can be used for reinforced concrete with rebar layer model. The model comprises of an isotropic hardening yield surface in the compressive field and a crack detection surface, which notifies if a node fails by cracking [10]. The two surfaces are independent. The stress-strain relationship for concrete under compression is taken by the EC2 formula. When a crack is detected, it is stored for the following computations, which are affected since a damaged elasticity model is used. The constitutive computations are made for each integration point of the model and the presence of the cracks modifies the material stiffness in that particular point. The crack can open and close. To define the shape of the failure surface of the concrete model, four failure ratios need to be defined. The ratio between the ultimate biaxial compressive stress and the ultimate uniaxial compressive stress is 1.16; the absolute value of the ratio of the uniaxial tensile stress at failure to the ultimate uniaxial compressive stress is 0.09; the ratio of the magnitude of a principal component of plastic strain at ultimate stress in biaxial compression to the plastic strain at ultimate stress in uniaxial compression is 1.28; the ratio of the tensile principal stress at cracking, in plane stress, when the other principal stress is at the ultimate compressive value, to the tensile cracking stress under uniaxial tension is 1/3. This model uses a softening relation between stress and strain after the failure of the concrete in the tensile field. In this case the interaction of the rebar layer with the concrete provides an amount of tension stiffening. It can be assumed that after the failure the stress reduces to a nil value linearly and reach a total strain of about 10 times the strain at failure [10]. The strain at failure tensile stress of the concrete is about $10^{-4}$, therefore, a total strain of $10^{-3}$ is assumed when the tensile stress reduces to zero.

**Element types**

Three element types have been used for this project. Shell elements are set for the concrete slabs and webs of the box section, beam elements model the tendons and gap elements are used for modelling the interaction between the concrete box girder segments. All the elements are deformable except for the gap elements. The thickness of the top slab, bottom slab and webs of the concrete box girder is very small compared with their width and length. Therefore, the shell element in the three-dimensional space is the most suitable element type for this case. The element type S4 is used for the shell parts of the structure. Rebar layer is used to provide reinforcement to the shell elements. The reinforcing steel is used for the material, with 24.2 mm diameter of the rebars, 10 cm of spacing between them and positioned in the middle of the thickness. Two layers of rebar reinforcement have been

assigned to the section. They are mutually orthogonally aligned to the edges of the shell element composing a square mesh. In case of non-linear analysis, the deformation of the underlying shell determines the deformation of the rebar layer. The reinforcement in the web segment where the tendons are anchored is increased for converging the solution and not to cause the failure in these points. The tendons are modelled with three dimensional beam elements. It consists in a wire element between two nodes. A linear integration with just one integration point is chosen since only normal force is acting in the tendons. The element type is called B31. A solid circular section is set for the tendon. The tendons that run along the whole span of the bridge are modelled together in one single tendon. A graphical representation is visible in figure 2. The cross section area of the tendon 19T15 composed by 19 strands of 15 mm diameter is 2850 $mm^2$, while the tendon 12T15 with 12 strands of 15 mm diameter has a cross section area of 1800 $mm^2$ [8]. The modelled long tendons have a radius of 67 mm, while for the short ones it is 24 mm. The tendons are modelled on the plan of the webs. This is a simplified model, however, in reality the tendons are also deviated in transversal direction.

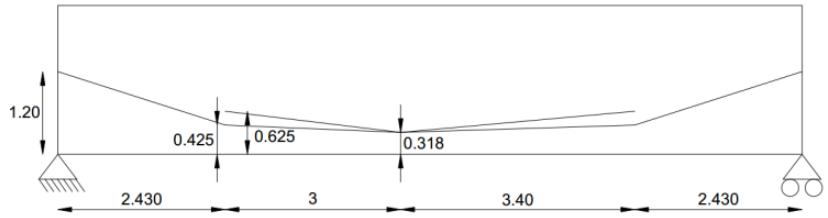


Figure 2 Longitudinal tendon layout with all dimensions in metres

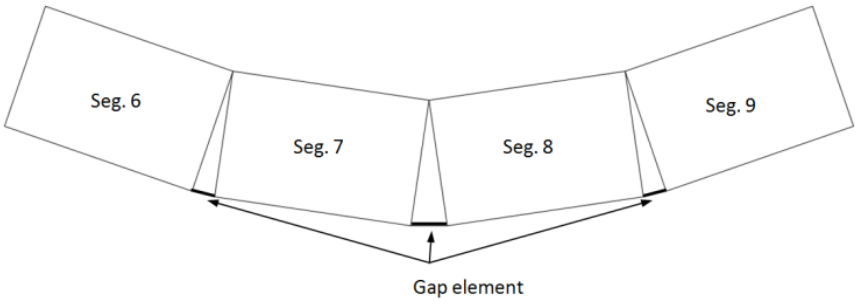


Figure 3 Mid-span segments with gap elements

The interaction between the segments of the bridge has been modelled by using gap elements. Since the slabs and the webs are modelled with shell elements, the interaction between the segments consists only between the edges of the shell and not on a surface interaction, as it would be in reality. For mechanical contact between two nodes GAPUNI elements are chosen. The contact behaviour is defined by the initial separation *d* of the gap and the direction of the contact **n**. During the loading of the bridge the deflection increases and the keys open starting from the bottom slab. Hence, the rotation around the top slab is allowed in the model (see figure 3). Considering that the segments of the bridge have different rotation from each other, a fixed direction of the gap element cannot be used. To allow the rotation of the gap element, only the distance *d* is defined in the model. The initial separation distance is set for obvious reason equal to zero since the joint is closed at the beginning. The mesh corresponds to the partition and the nodes created, therefore, in the size control for the mesh definition the unit value is introduced.

## Constrains and Boundary Conditions

The boundary conditions applied in the model are the bridge supports at the end segments and the fixed transversal movement of the tendons at the deviation points. The three translations on one end bearing are fixed, while on the opposite end only longitudinal displacement is allowed. This condition is usually designed in real bridges in order to take into account the displacement due to creep, shrinkage and temperature variation. Four supports are set and the other two have only fixed vertical displacement. The rotation is allowed in all directions. The tendons are anchored to the concrete with tie constraints. The end nodes of the tendons are constrained to have the same motions of the anchorage nodes in the concrete, in other words, of the master nodes. As regards to the tendon deviated points, they are fixed in transversal direction and free to move vertically with the deviator block. Due to the high difficulty of modelling the frictional behaviour of the tendon inside the deviator block, one of these two extreme models has to be chosen: the tendon is blocked with the deviator or the tendon is free to slip. Since one of the required output is the tendon slip, the longitudinal movement of the tendon at the deviated point is allowed. This assumption causes a lower ultimate load and better approximates the stress increment in the tendons [6]. To create the interaction between the tendon and the deviator segment in the way that the tendon moves downwards when the bridge deflects, the multi-point constraint (MPC) of type “link” is used in the model. This constrain is a linear constrain between two nodes selected and provides a pinned rigid link to keep fixed the distance between them. The rigid wire links the deviated points of the tendons to its projection on the centroid level. Figure 4 represents the constraint assumed. In this manner the tendon can freely slip, but it has to deflect as well as the full bridge does.

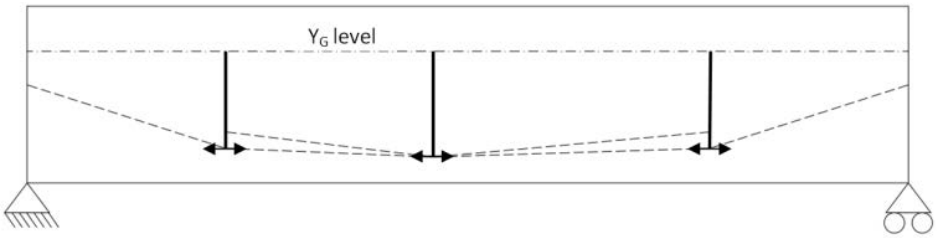


Figure 4 Allowed movement of the tendon at the deviated points

## Load Steps

The initial step is created automatically when the model starts. In this step, the boundary condition and the prestressing force are involved. The load is applied in two further separate steps. The total prestressing computed from back calculation by Takebayashi et al. is 38443 kN. The sum of the cross section areas of 10 tendons 19T15 and 2 tendons 12T15 is 32100 $mm^2$. Hence, the stress in the tendons results to be 1197.60 MPa. In Abaqus the initial stress field is defined to apply the prestress. It is applied uniformly over the beam elements. A local coordinate system is given to the tendons in such a way that the direction of the stress applied can be easily recognized. The first step is a general static step that includes the prestressed force and the dead load. During this stage the materials are still in elastic state and the displacement is small. Therefore, the modified Newton method is sufficient for this step. However, the geometric nonlinearity is activated since this step and it needs to be switched on for the next one when large displacements and material nonlinearity occur. The initial and maximum increment is set equal to 0.1. The dead load is modelled as body force applied to the slabs and webs in vertical direction with a value of 25000 $N/m^3$, which is conventionally

taken as the specific weight for reinforced concrete. During the second step, a static Riks method has been used which is useful to predict unstable, geometrically nonlinear collapse of a structure [10]. This method considers both load magnitude and displacement as unknown. To solve the problem Abaqus uses the “arc length” method. This method is independent from the response, which can be both stable and unstable. The multiple loads applied on the structure are increased and have the same magnitude till the collapse. The solution of load magnitude and displacement are found simultaneously. The method adopted in this paper is based on the Newton one. The load applied in the second step is simplified with respect to the one applied in a real bridge. The distributed load over the top slabs of the six segments 4, 5, 6 and 9, 10, 11 is divided into concentrated forces on the top web nodes of the joints.

## MODEL VALIDATION

The numerical model established in this study is validated by comparing the results optained from the model with the experimental ones in the following aspects.

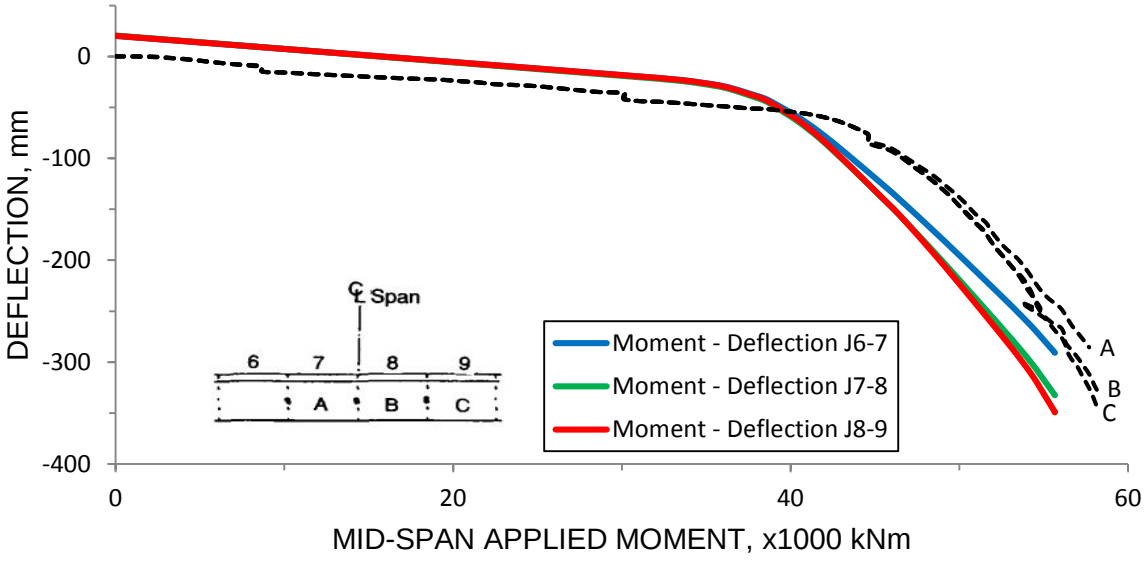


Figure 5 Deflection at the mid-span joints from numerical analysis and experimental test [5]

### Deflection

The load-vertical displacement curve is plotted in figure 5. Deflection is related in the 3 central joints at the height of 1.20 m from the bottom slab of a concrete box girder segment. The plot has a similar trend with the graph provided by Takebayashi from measurement [5]. The modelled bridge fails at a lower load than the real case. This is due to the assumption of free slipping tendon at the deviator points made during the modelling. In fact this leads to a lower ultimate load as it stands in Ramos and Aparicio [6]. The bridge is initially uplifted because of the prestressing force and, therefore, has a positive vertical displacement of about 2 cm. Both graphs have a linear behaviour till the applied midspan moment reaching about 40000 kNm. In the experimental case the local variations is the result of temperature change [5], while in the current model this is not taken into consideration.The maximum vertical displacement in the model, 34.9 cm, is achived in the joint between the segments 8 and 9 while the midspan joint deflection is 33.3 cm. The asymmetric disposal of the tendons causes a lower vertical displacement at the joint between segments 7 and 8.

**Joint Opening**

The joint opening between segment 8 and 9 is plotted for different heights from the bottom slab: 1.60 m, 1.20 m, and 0.318 m. The trend of the joint opening versus the midspan applied load is shown in figure 6 for the modelled bridge and for the experimental one. Also, in this case the results are similar except for the load from which the joint starts opening and ultimate load reached. The difference is due to the same reason explained previously. In the model the joint 8-9 starts to open from the bottom, the node at the height 0.318 m from the bottom slab is the first that opens at the loading of 35000 kNm. In the experimental study the same node starts to open at about 40000 kNm. Other two nodes at height 1.20m and 1.60m start to open slightly later and reach respectively a total gap of 17.1 mm and 7.7 mm when the bridge collapse, while the final opening of the lower node is 33.8 mm.

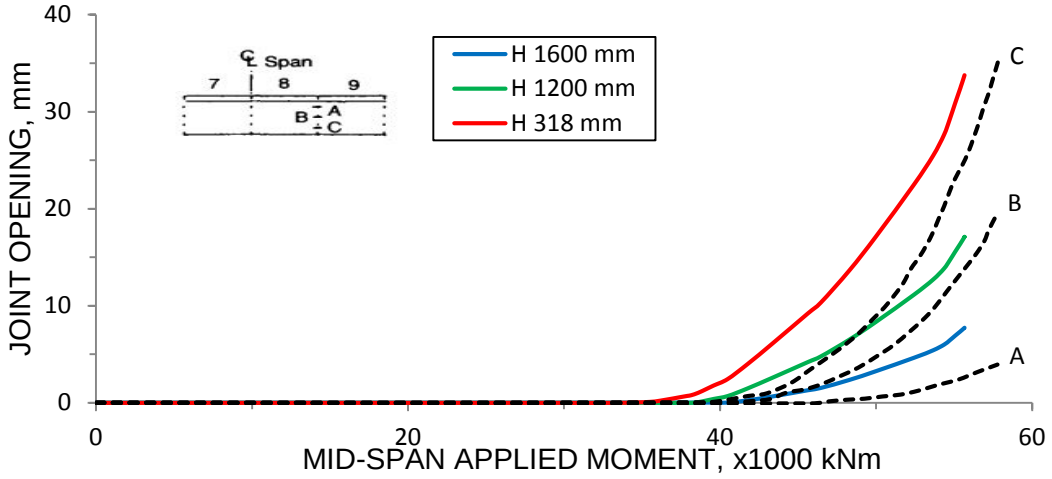


Figure 6 Opening of the joint 8-9 versus mid-span moment from numerical analysis and experimental test [5]

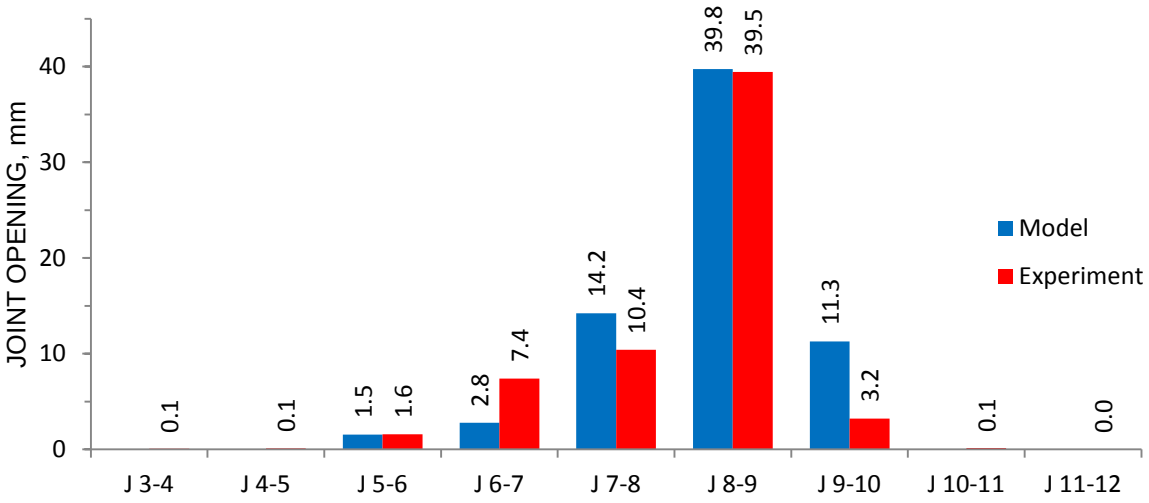


Figure 71 Opening of the joints from numerical analysis and experimental test [5]

The opening is also analysed at the bottom of the web for each joint and plotted in figure 7 from numerical analysis and experimental test. The largest openings are found nearby the mid-span, with the maximum opening at the joint 8-9 of 39.8 mm. The opening values decrease when moving away from the mid-span joint. The joint between segments 6 and 7 has larger opening than the one between segments 9 and 10 in the test, while it is the reverse in the model.

**Tendon Slip**

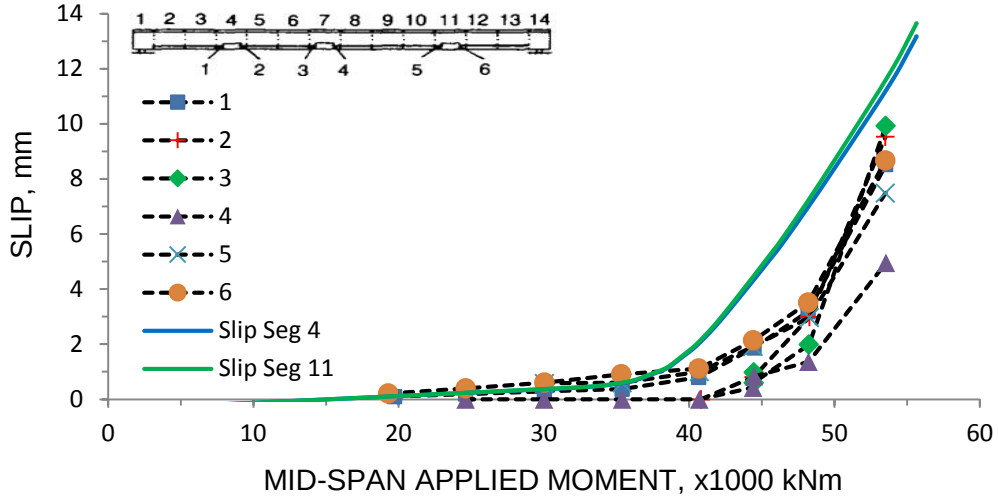


Figure 8 Slip of the long tendon from numerical analysis and experimental test [5]

The tendon slip from numerical analysis are compared with those from experiment. The assumptions made in the model lead to the results of tendon slips shown in figure 8 and figure 9 from numerical analysis (continuous lines) respectively for the long and short tendons. The slip at segments 4 and 11 is related to the whole span tendons, while the slip at segment 7 is related to both types of tendons since they are deviated in the same point. The slips are about 13 mm on the side deviators and about 22 mm in the central deviator.

Comparing the results with those provided by Takebayashi for the tendon 5 and tendon 6 (dashed lines) in figure 8 and figure 9 one can see that the tendon slip from numerical analysis has higher value. For the tendon 5, which runs for the whole bridge, the slips are between 7 mm and 10 mm. In the tendon 6, which has only one deviator at the segment 7, the slippage is about 5.5 mm. This result is very small compared with the value obtained from the numerical analysis in the same deviator. The reason is because the two nodes of the tendons are coupled and the applied prestressing forces are higher in the central deviator node of the model. In order to compare with the tendon slip obtained from numerical analysis, the slippage of the two tendons in the experimental test has to be summed. Hence, a total tendon slip displacement of about 15.5 mm from experiment can be compared with the 22 mm obtained from numerical analysis. The numerical value is larger in any case for every deviator segment and this is due to the free slipping assumption previously mentioned. The slip at the deviators occurs since the beginning of the loading step because of no friction supposed, while in reality the tendons start to move at different load values according to their deviation angle. One can notice that the movement is small during the linear stage and large slippage starts to occur at the loading level between 40000 and 45000 kNm. This behaviour is

observed also in the model but with big displacement starting from about 38000 kNm due to no friction assumption made.

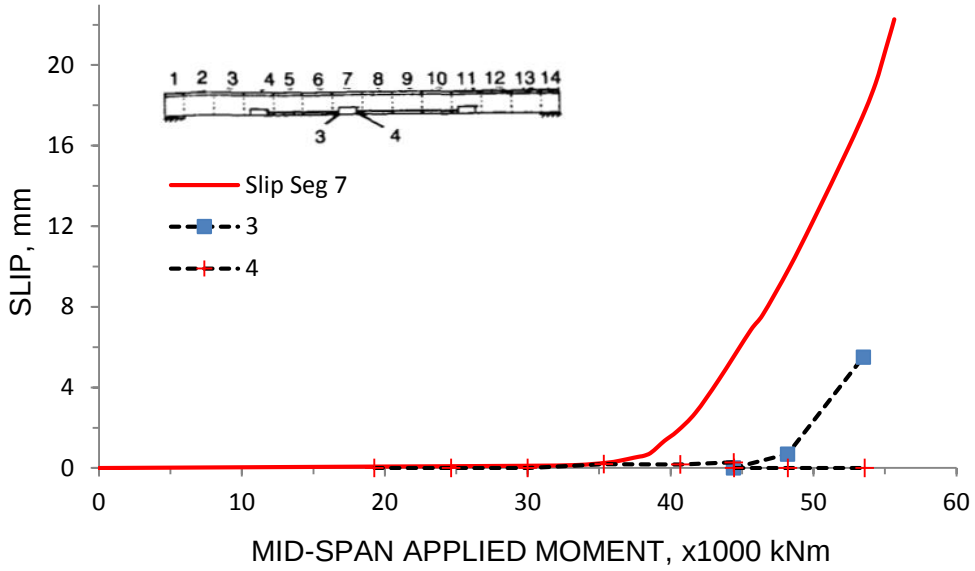


Figure 9 Slip of the short tendon from numerical analysis and experimental test [5]

## SUPPLEMENTAL RESULTS

Some further results of the current study are discussed for better understanding of behaviours of externally prestressed precast segmental bridges with dry joints. Such results as stresses in the concrete and tendons are not obtained from the real test.

### Concrete Stress

The stress in the concrete is plotted for different load steps. In figure 10 it is related to the stage where only the dead load and the prestressing force are applied. It corresponds to the initial condition when the load magnitude is $\lambda = 0$. The vertical displacement is scaled for the factor 20. The bridge is all in compression, except for the end segments where small tensile stress occurs due to the anchorage of the tendons. The maximum compression value is at midspan intrados equal to about 13 MPa.

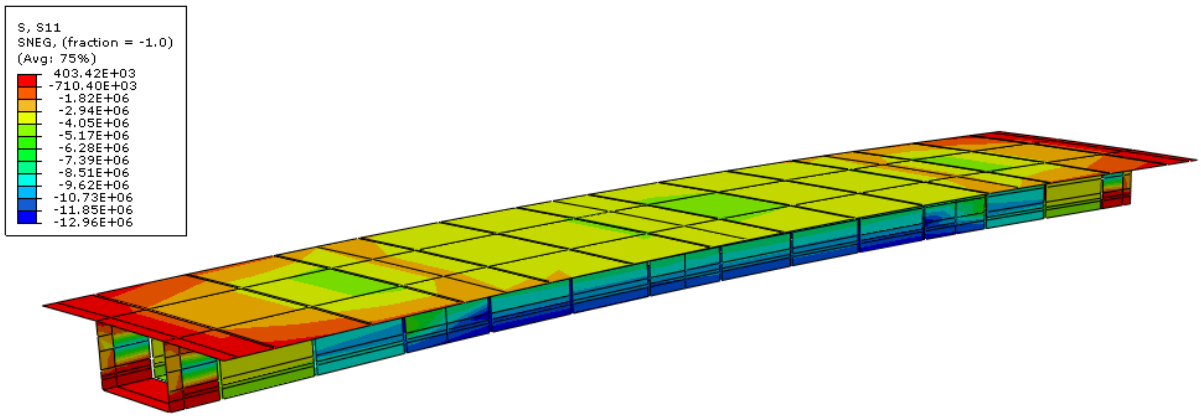


Figure 10 Concrete stress under prestressed force with all dimensions in Pa

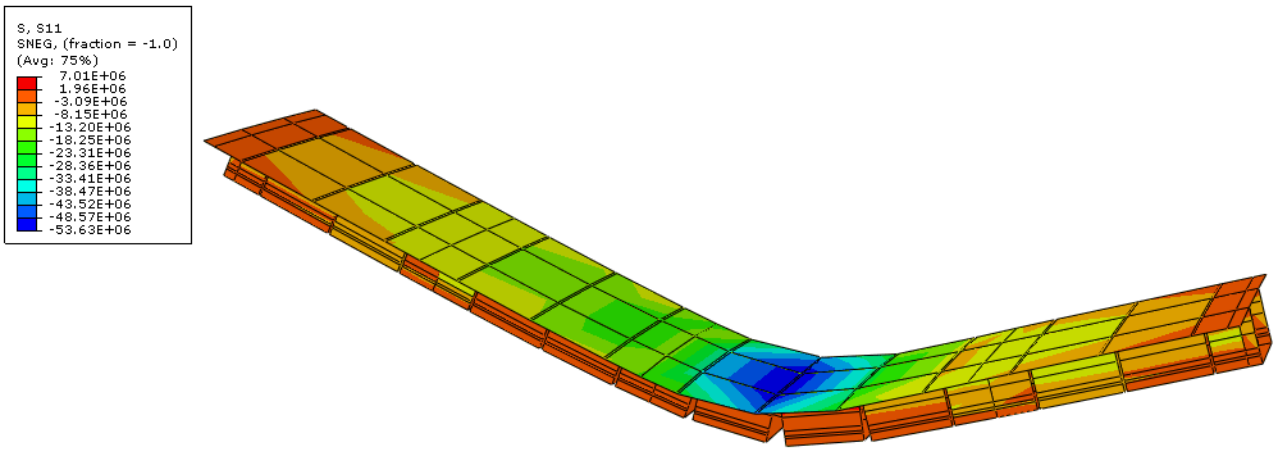


Figure 112 Concrete stress at ultimate load with all dimensions in Pa

The concrete stress at the ultimate load is represented in figure 11. The bridge collapses at the applied midspan bending moment of 55658 kNm. The total applied load on the bridge is 8481 kN. The bridge fails for compression of the top slab, in fact, the stresses reach a value of 53 MPa at the joint 8-9.

**Tendon Stress**

The stresses of the tendon between the ends of the bridge are presented in figure 12, while those of the tendon between the two lateral deviators are shown in figure 13. The initial stress was 1198 MPa and uniformly distributed in both tendons.

The stresses in the long tendon at ultimate load vary from 1429 MPa at the anchorage in segment 1 to 1450 MPa at the central part. The increment is respectively of 231MPa (19%) and 252 MPa (21%). The higher stresses in the central part are due to the larger deflection and concentration of joint opening nearby the mid-span of the bridge. The stresses in the short tendon are 1672 MPa in the part between the segment 4 and 7, while 1602 MPa in the part between segment 7 and 11. They increase respectively of 474 (40%) and 404 (34%) from the initial condition.

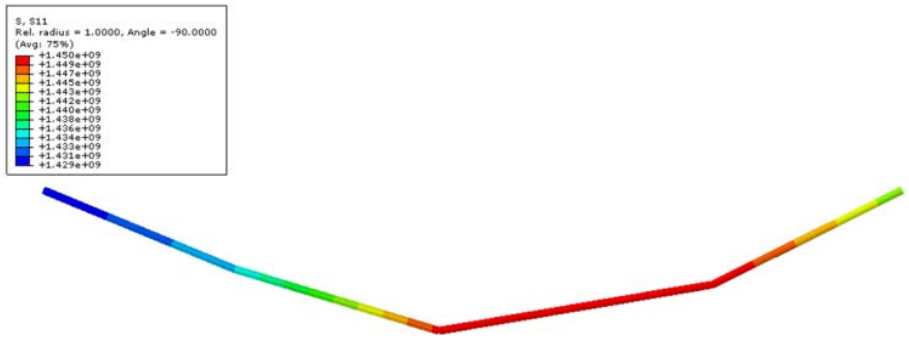


Figure 123 Long tendon stress at ultimate load

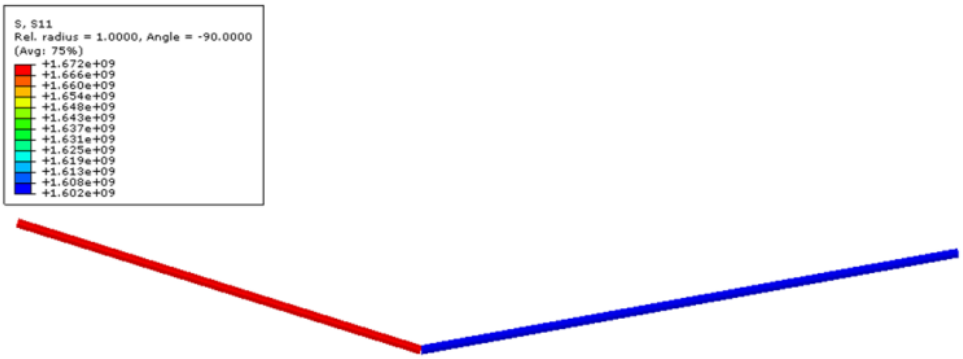


Figure 13 Short tendon stress at ultimate load

## CONCLUSION

The behaviour of the precast concrete segmental bridge with external tendons and dry keyed joints is linear in the first loading stage followed by a non-linear one where large displacements occur. All the joints remain close till when about 30000 kNm mid-span moment is applied and all the segments are still in compression. The deflection of about 2 cm at the mid-span of the bridge is also small for this load level. The bridge collapse at 55658 kNm applied midspan moment for flexural failure as experienced during the real test. Crushing of the concrete in the top slab creates a hinge in the midspan and generates the mechanism. The non-linear analysis used in the model well performs the real behaviour of the tested bridge. At the final load level the deflection reaches 35 cm and the opening is 40 mm at joint between segment 8 and 9. The deflection is not symmetric since the layout of the prestressing steel is asymmetric. Considerable warning is given by the large displacements occurred. A higher assumption of concrete strength may increase the loading capacity of the structure. However, a lower ultimate load was expected since no friction was assumed between the tendons and the deviator blocks. If fixed tendon model at the deviators is applied, the structure fails at higher load and the increment of tendon stress is not significant. Better resulting model would be obtained if friction interaction would be used between the nodes of the tendons and those of the concrete at the deviation points.

Concerning the ultimate limit state design, the model does not reach its design limit because of the assumption of free slipping of the tendons. This assumption can be adopted in favour of safety for the design at ULS. If the slippage is denied, the tendon force increases in the central part and the neutral axis drops. Therefore, increasing the friction between the ducts and deviator blocks improve the loading capacity of the structure.

## REFERENCES

1. POSTON, R W, WOUTERS, J P. *Durability of Precast Segmental Bridges*, NCHRP Web Document 15, National Cooperative Highway Research Program, June 1998, http://www.nap.edu/readingroom/books/NCHRP15/front.html.

2. WIUM, D J W, BUYUKOZTURK, O. *Precast Segmental Bridges - Status and Future Directions*, Civil Engineering for Practicing and Design Engineers, ACSE, V. 3, 1984, pp 59-79.

3. ZHOU, X, MICKLEBOROUGH, N, LI, Z. *Shear strength of joints in precast concrete segmental bridges*, ACI Struct. J., 102(1), 2005, pp 3–11.

4. SHAMASS, R, ZHOU, X, ALFANO, G. *Finite-Element Analysis of Shear-Off Failure of Keyed Dry Joints in Precast Concrete Segmental Bridges*, ASCE J. Bridge Eng., 2014, pp 1-12

5. TAKEBAYASHI, T, ET AL. *Full-scale destructive test of a precast segmental box girder bridge with dry joints and external tendons*, Proceedings of The Institution of Civil Engineers Structures and Buildings, 1994, pp 297-315

6. RAMOS, G, APARICIO, A C. *Ultimate Analysis of Monolithic and Segmental Externally Prestressed Concrete Bridges*, Journal of Bridge Engineering, ACSE, V. 1, No. 1, 1996, pp 10-17

7. TANDLER, J. *Collapse analysis of externally prestressed structures*, 2009, Diplomica Verlag

8. DEBERNARDI, P G. *Strutture di calcestruzzo armato e precompresso*, 2011, Celid

9. ABAQUS 6.14-4. *Computer software*. Waltham, MA, Dassault Systèmes

10. ABAQUS Documentation 6.14. *Abaqus Analysis User's Guide*

11. EN 1992-1-1. *Eurocode 2: Design of concrete structures – Part 1-1: General rules and rules for buildings*, 2004

12. TURMO, J, RAMOS, G, APARICIO A C. *FEM study on the structural behavior of segmental concrete bridges with unbounded prestressing and dry joints: Simply supported bridges*, Engineering Structures, 27, 2005, pp 1652-1661

13. EN 1992-2. *Eurocode 2: Design of concrete structures – Part 2: Concrete Bridges – Design and detailed rules*, 2005